THERMAL ISSUES FOR THE OPTICAL TRANSITION RADIATION SCREEN FOR THE ELI-NP COMPTON GAMMA SOURCE

F. Cioeta†, D. Alesini, A. Falone, V. Lollo, L. Pellegrino, A. Variola, INFN-LNF, Frascati, Italy
D. Cortis, M. Marongiu, V. Pettinacci INFN-Roma, Roma, Italy
A. Mostacci, L. Palumbo, M. Ciambrella, Rome University La Sapienza, Roma, Italy

Abstract

A high brightness electron LINAC is being built in the Compton Gamma Source at the ELI Nuclear Physics facility in Romania. To achieve the design luminosity, a train of 32 bunches, 16 ns spaced, with a nominal charge of 250 pC will collide with a laser beam in two interaction points. Electron beam spot size is measured with Optical Transition Radiation (OTR) profile monitors. In order to measure the beam properties, the OTR screens must sustain the thermal and mechanical stress due to the energy deposited by bunches. This paper is an ANSYS study of the issues due to the high energy transferred to the OTR screens. Thermal multicycle analysis will be shown; each analysis will be followed by a structural analysis in order to investigate the performance of the material.

INTRODUCTION

The Gamma Beam Source (GBS) machine [1] is an advanced source of up to ≈ 20 MeV Gamma Rays based on Compton back scattering, i.e. collision of an intense high power laser beam and a high brightness electron beam with a maximum kinetic energy of about 740 MeV. The nominal electron beam consists in trains of 32 electron bunches 250 pC each, separated by 16 ns, distributed along a 0.5 μs RF pulse, with a repetition rate of 100 Hz. In order to measure the beam profile, Optical Transition Radiation (OTR) target are used. Such technique is common in conventional [2] and unconventional [3,4] high brightness Linacs. For the ELI-GBS, Aluminium or monocrystalline silicon are the target material under investigation. The radiation is emitted when a charged particle beam crosses the boundary between two media with different optical properties (i.e. different dielectric constant). This radiation hits the screen for several cycles during the experiments. The outcome of previous analysis [5] has been used as input for finite element study in order to assess the thermomechanical features of both materials, especially under high number of thermal cycles.

FINITE ELEMENT SIMULATIONS

The 100 Hz impacts of the electron beam on the OTR target produce a continuous oscillating change of the temperature distribution. In order to evaluate the spatial and temporal evolution of this distribution during the heating and the cooling (thermal cycle) of the OTR target several thermal transient analyses have been performed. The high number of impacts of the beam on the target and the particular geometry of the beam spot size, led to simulate a high number of cycles, by means of a dedicated finite element code in ANSYS APDL [6]. Once calculated the temperature evolution over the time of the OTR screen, the equivalent Von Mises stress state [7] has been obtained for the steady temperature reached during the heating (ANSYS first load step [6]) and the cooling (ANSYS second load step [6]) of the first thermal cycle evaluated as the most severe test situation. Therefore, in order to assess the OTR screen performance, the fatigue damage and the number of cycles to failure have been calculated applying the theory of Wohler, Goodman and Miner [7]. The main properties for aluminium (Al) and monocrystalline silicon (Si) assumed in the finite element simulations are reported in Table1.

Table 1: Material Properties [8]

	Al	Si
Young's Modulus	69 GPa	150 GPa
Poisson	0.33	0.17
Density	2,700 kg/m^3	2,330 kg/m^3
Coefficient of Thermal Expansion	23 x 10^{-6} K^{-1}	2.5 x 10^{-6} K^{-1}
Thermal Conductibility	209.0 W/m/K	14.5 W/m/K
Specific Heat Capacity	890 J/kg/K	700 J/kg/K

THERMAL TRANSIENT ANALYSIS

The geometry of the OTR target (30 mm of length for each edge and 1 mm of thickness) was modelled with 3D SOLID70 elements [6]. A refinement of the mesh (see Fig. 1, darker area) was applied close to the electron beam spot where is concentrated the heat generation (minimum size of the mesh elements 6 x 10^{-6} m). The ANSYS APDL code applies the thermal load to the mesh elements corresponding to the OTR target portion significantly interacting with the electron beam. It was considered an elliptical beam spot corresponding to the most possible focused beam, which represents the worst-case scenario (see Fig.1 and Table 2).

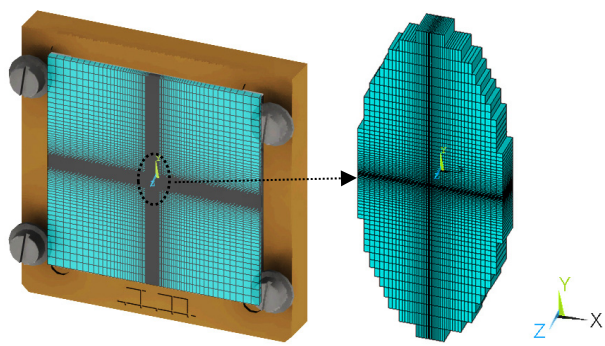

Figure 1: OTR screen and Hotspot 3D Mesh.

† fara.cioeta@lnf.infn.it

The thermal power, that represents the heat generation due to the interaction between the target and the electron beam, is applied on the hotspot elements by means of a Gaussian distribution (see Fig.2). The distribution has been calculated through the coordinates of the centroids (x,y) of the mesh elements and the beam properties (Table 2). Moreover, Figure 2 shows the comparison between the two-dimensional Gaussian distribution calculated with the theoretical formula [9] and the thermal power distribution extracted from the elements of the mesh and applied by the ANSYS APDL code.

Table 2: Beam Properties

	Data
Beam Sigma along x-axis (rms)	47.5 x 10^{-6} m
Beam Sigma along y-axis (rms)	109.0 x 10^{-6} m
Bunch Charge	250 x 10^{-12} C
Bunch Pulse	32
Bunch Spacing	16 x 10^{-9} s
Pulse Distance	1.00 x 10^{-2} s
Pulse Length (rms)	5.12 x 10^{-7} s
Number of Electron in a Pulse	4.99 x 10^{10}
Electron Stopping Power (Aluminium)	8.65 x 10^{-11} J/m
Electron Stopping Power (Silicon)	7.47 x 10^{-11} J/m
Peak of Thermal Power	2.2 x 10^{14} W/m^3

The first thermal boundary condition applied to the OTR screen, is the initial temperature of 295.15 K for all nodes of the mesh, corresponding to GBS room temperature. An additional boundary condition is the fixed temperature of 295.15 K along the OTR target edges in contact with the frame support and the screws (see Fig.1).

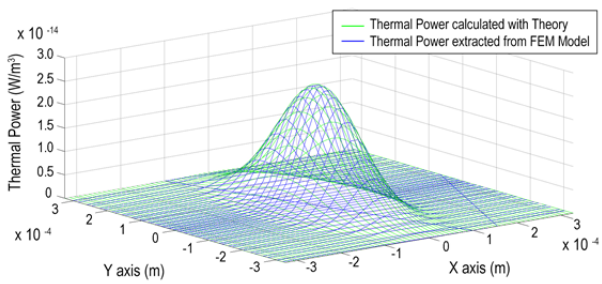

Figure 2: Thermal Power on the Elements of the Hotspot.

Figure 3 represents the spatial thermal distribution (x,y) at the peak temperature in the beam hotspot for both materials, while Figure 4 shows the trend of temperature after 0.001 s. The silicon has a higher and a more spatially concentrated ΔT respect to the aluminium. The aluminium has a higher specific heat capacity and thus a lower maximum temperature than the silicon for the same amount of deposited beam power. In order to evaluate the number of cycles needed to reach constant temperature a dedicated transient analysis have been set through the ANSYS APDL code (600 thermal cycles). The results are reported in Table 3 and Figure 4, where it is evident the different maximum temperature achieved and the trend of the OTR cooling. The steady maximum temperature for the aluminium is reached after 80 cycles (0.8 s) and is equal to 345.3 K, whereas for the silicon is reached after 92 cycles (0.92 s) and is equal to 358.9 K. The results are rounded off to one tenth of K. The different steady maximum temperature of two materials is due to different specific heat capacity as well.

Table 3: Temperature (Al, Si) of the Hotspot Elements

Material	Max. Temp.	Min. Temp.
Aluminium	345.3 K	296.1 K
Silicon	358.9 K	296.3 K

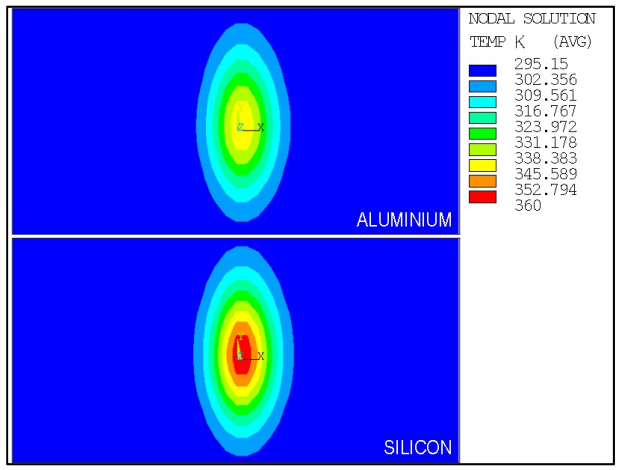

Figure 3: Temperature spatial distribution (Al, Si).

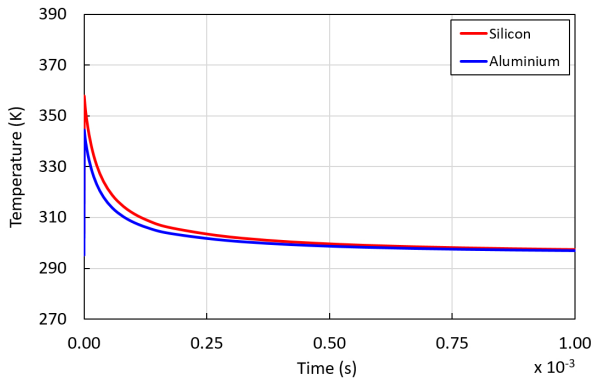

Figure 4: Thermal transient analysis (Al, Si).

STATIC STRUCTURAL ANALYSIS

Starting from the results of the thermal transient analysis, the OTR screen mechanical performance for both materials has been evaluated with a dedicated static structural analysis. The nodal thermal distribution, after the heating and the cooling of the first thermal cycle of transient simulations, was the input for a linear static solution.

Figure 5 represents the contour plot of the Von Mises equivalent stress distribution. The maximum stress is located in the central element of the hotspot where there is the hottest point of the OTR screen. The aluminium has a maximum equivalent stress of 53.90 MPa, while the silicon has a maximum equivalent stress of 12.02 MPa, both under the yield limit. The maximum displacements

ISBN 978-3-95450-182-3

due to the equivalent stress values is reported in Table 4. Despite of the greater ΔT, the silicon has achieved the best mechanical performance under the heat generation of the electron beam.

Comparing the geometrical distribution on the XY plane (i.e. the OTR screen plane - see Fig. 6) of the displacement vector sums, it is evident the better performance of the silicon with respect to aluminium. A high distortion of the OTR screen surface close to the electron beam hotspot could generate a loss of image resolution [10]. For a generic monocrystalline silicon plate, the production mean square roughness is under 1 x10^{-9} m. Therefore, the evaluation of the OTR screen strain surface is relevant for its optical performance. In this case, for the silicon we obtained a maximum displacement of 15.9 x10^{-9} m, one order of magnitude greater than the production tolerance for the silicon plates.

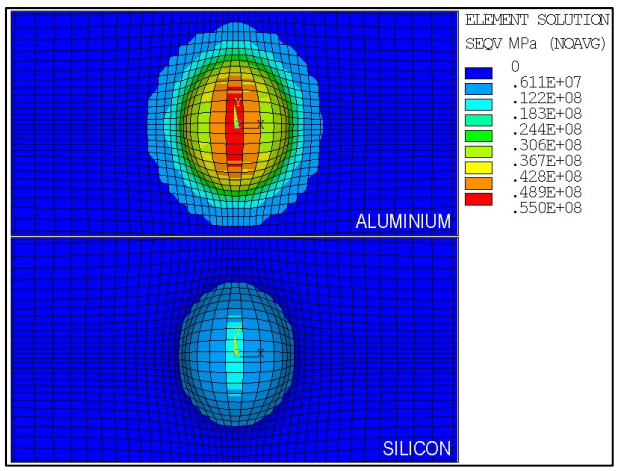

Figure 5: Equivalent Von Mises Stress (Al, Si).

Table 4: FEM Structural Analysis Results

	Al	Si
Max. Equiv. Stress	53.90 MPa	12.02 MPa
Min. Equiv. Stress	0.13 MPa	0.04 MPa
Max. Displacement	148.5 x10^{-9} m	15.9 x10^{-9} m

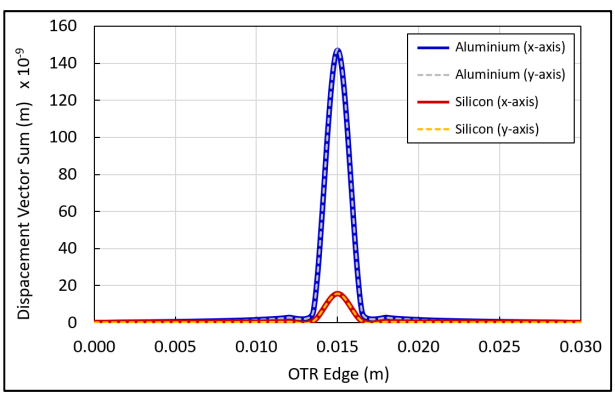

Figure 6: Displacement Vector Sum long x and y axes of the OTR Target (Al, Si).

FATIGUE ANALYSIS

Considered maximum and minimum equivalent stress obtained in the previous step, the fatigue damage and the number of cycles to failure for the both materials have been calculated applying the theory of Wohler, Goodman and Miner [7]. The fatigue analysis results are reported in Table 5. The aluminium reaches an alternate stress of 30.20 MPa while the silicon an alternate stress of 7.74 MPa. Considering the curve of Wohler for the aluminium [11] and for the silicon [12], after one operating hour the aluminium screen achieve a cumulative fatigue damage of 0.59, where 1.00 represents the failure.

Table 5: Fatigue Analysis Results

	Al	Si
Alternate Stress	30.20 MPa	7.74 MPa
Number of cycles to failure	609.700	∞
Cumulative fatigue damage after one operating hour	0.59	0.00

Reducing the number of bunches the fatigue behaviour of the aluminium changes completely. In fact, the rise of temperature decreases proportionally with the number of bunches (see Table 6): it turns out in a reduction of the equivalent stress and therefore a reduction of the alternate stress. For instance, halving the number of bunches there is an endless life for the aluminium screen as well.

Table 6: Temperature VS Bunches for the Aluminium

Number of Bunches	Max. Temp.	Alternate Stress	Number of cycles to failure
32	344.4 K	30.20 MPa	609,700
16	320.2 K	15.20 MPa	∞
8	307.7 K	n.a.	∞
4	301.4 K	n.a.	∞
2	298.3 K	n.a.	∞
1	296.7 K	n.a.	∞

CONCLUSION

This paper proposes a finite element thermal and structural analysis to identify the best solution for OTR screens under thermomechanical stress, such as in the ELI-NP GBS. We compared aluminium and silicon screens. The choice of the silicon, initially predicted by a preliminary theoretical analysis [13,14], is confirmed by the fatigue analysis based on the results of a static structural finite element simulation.

The next activities foreseen will shift the focus on the analysis of the mechanical supports and on the thermal contacts simulation, in order to evaluate their influence on the results (further thermal dissipation and mechanical stresses) that could degrade the performance of the whole OTR system. A more careful analysis will be devoted to the loss of image resolution due to silicon strain.

REFERENCES

[1] A. Bacci, D. Alesini, P. Antici, *et al.*, "Electron linac designto drive bright Compton back-scattering gamma-ray sources" *Journal of Applied Physics*, vol. 113, no. 19, p.194508, 2013.

[2] D. Alesini *et al*. "Status of the SPARC project". *Nuclear Instruments and Methods in Physics Research Section A, Volume 528, Issue 1-2, p. 586-590*, 10.1016/j.nima.2004.04.107.

[3] P.Antici *et al*. "Laser-driven electron beamlines generated by coupling laser-plasma sources with conventional transport systems". Journal of Applied Physics **112**, 044902 (2012); doi: `http://dx.doi.org/10.1063/1.4740456`

[4] A.R. Rossi *et al*. "The External-Injection experiment at the SPARC_LAB facility". *Nucl.Instrum.Meth. A740 (2014) 60-66*, 10.1016/j.nima.2013.10.063.

[5] F. Cioeta, *et al*. "Thermal Simulation for Optical Transition radiation screen for ELI-NP Compton gamma source". Proceedings of IBIC2016, Barcelona, Spain, paper TUPG75.

[6] ANSYS Inc., "ANSYS Mechanical APDL Theory Reference", *Release 15.0, November 2013*.

[7] J. E. Shigley, R. G. Budynas, J. K. Nisbett, D. Amodio (Translator), G. Santucci (Translator), "*Progetto e Costruzione di Macchine*", Mc Graw Hill.

[8] Material parameters taken by: `http://www.matweb.com/`

[9] Two-dimensional Gaussian function: `https://en.wikipedia.org/wiki/Gaussian_function`

[10] Marc Ross, et al. "A Very High Resolution Optical Transition Radiation Beam Profile Monitor". *Proceedings of BIW02*, Upton, New York, U.S.A.

[11] G. T. Yahr, "Fatigue Design Curves for 6061-T6 Aluminium". *Engineering Technology Division, Oak Ridge National Laboratory, Oak Ridge, Tennessee 37831-8051.*

[12] M. J. Kirkham. "Advances in Ultra-High Cycle Fatigue". University of Tennessee, Knoxville.

[13] M. Marongiu *et al*., "Thermal behaviour of the optical transition radiation screens for the eli-np compton gamma source", Nuclear Instruments and Methods in Physics Research Section A: Accelerators, Spectrometers, Detectors and Associated Equipment, 2016 doi: 10.2016/j.nima.2016.07040

[14] M. Marongiu *et al*. "Design issues for the optical transition radiation screens for the ELI-NP Compton Gamma Source". Proceedings of IPAC2016, Busan, Korea, paper MOPMB017.

ISBN 978-3-95450-182-3